Iranian Journal of Chemistry and Chemical Engineering (IJCCE)

A Comparative Study on the Performance of Polyaniline-Silica and Reduced Graphene Oxide-Silica Nanocomposites to Oil-Water Emulsion Separation

Davoud Babakhani[1]*, Masoud Hamidi[2]

[1]R&D Department of Arak Oil Refining Company, Arak 3867141111, Markazi, Iran

[2]R&D Department of Arak Petrochemical Company, Arak 3867143111, Markazi, Iran

[*]E-mail address: engbabakhani@gmail.com

[2]E-mail address: hamidi.m1983@gmail.com

ABSTRACT: *Oily water is one of the most common issues, which is attributed to the petroleum industry in the form of oil-water (O-W) emulsion. Therefore, it is necessary to treat it before being released into the environment. In this study, the possibility of two different nanocomposites has been investigated in the demulsification of O-W emulsions. First, silica (SiO_2) nanoparticles and graphene oxide (GO) nanosheets were synthesized using the sol-gel process and the Hummers' method, respectively. Next, polyaniline (PANI)-silica and reduced graphene oxide (rGO)-silica nanocomposites were synthesized by applying in situ chemical oxidative polymerization and sol-gel processes, respectively. EDX analysis showed the proper reduction of GO to rGO nanosheets. In addition, SEM results revealed that the PANI-silica nanocomposite was more functional compared to rGO-silica due to its higher specific surface area and higher demulsification efficiency. Accordingly, bottle tests and optical microscopy images proved that the adsorption capacity of PANI-silica nanocomposite is greater than that of rGO-silica nanocomposite. Furthermore, the demulsification results indicated that the optimum adsorption percentage of oil from the O-W emulsion corresponded to the oil content in the emulsion and was not correlated to the nanocomposite type. It was figured out that the performance of nanocomposites was better when using less oil in the O-W emulsion. BET analysis also showed that the surface area of PANI-silica was two times greater than that of eGO-silica, which caused better O-W emulsion separation. The hydrophobicity observations confirmed that the surface of PANI-SiO_2 can absorb more oil droplets compared to rGO-SiO_2. Last, the possible mechanism of demulsification by applying nanocomposite as an adsorbent was also explained.*

KEYWORDS: *adsorbent, Polymer nanocomposite, oil-water treatment, reduced graphene oxide, polyaniline*

INTRODUCTION

The oil-in-water (O-W) emulsion produced by the petroleum industry is stable, and the separation processing is difficult, which has received sustained attention for decades [1-5]. The extremely stable emulsion generates significant issues in the downstream process, such as contaminated water [5]. In this case, the development of a high-performance demulsifier for the remediation of contaminated water with oil is crucial. There are several methods to expedite the demulsification process of O-W emulsion, such as thermal, mechanical, electrical, and chemical methods, of which the chemical method is the preferred process due to its high efficiency and facile operation [6-8]. In the last few decades, researchers have investigated highly efficient and low-cost demulsification materials to break the O-W emulsion under ambient conditions. For this purpose, different chemical demulsifiers such as block copolymers, polysiloxane, dendrimer, and ionic liquids were developed [9-14]. Due to environmental protection, the practical application of these chemical demulsifiers has been restricted [15].

Most separation technologies, such as gravity separation, membrane separation, air flotation, etc. are expensive, highly costly, energy-intensive, complicated, and time-consuming. In recent decades, the application of nanomaterials to environmental and medical issues has obtained extensive interest.

Some researchers have synthesized nanoparticles and nanosheets such as silica oxide, graphene oxide, reduced graphene oxide, and titania to remedy oily water [16-20]. Recently, graphene oxide (GO) has attracted great interest in O-W emulsion separation applications.

In the form of graphene sponge and mesh, graphene is often used to absorb or filter oil due to its low surface energy, low density, and high surface area. The introduction of the functional groups of carbonyl, hydroxyl, and ethoxy on the edges of GO makes it a good amphipathic surfactant with hydrophilic edges and a hydrophobic basal plane. Therefore, the functionalized GO might find an important application in the demulsification of the O-W emulsion.

It is well-accepted that GO nanosheets contain a high content of hydrophilic oxygen-containing groups [21]. The nature of the GO nanosheets is hydrophilic due to their polar oxygen functional groups, which cause a proper and stable dispersion in many solvents, such as water. Although the hydrophilicity of the GO nanosheet can be a positive factor in the separation of oil from O-W emulsion, it was observed that the separated water still contained a percentage of oil and GO [22]. This demerit can be modified by applying some hydrophobic nanoparticles, such as SiO_2 nanoparticles. SiO_2 nanoparticles have broadly been used as surface-modified nanoparticles to enhance the hydrophobicity property of nanocomposites [23, 24]. In addition, polymer nanocomposite membranes have been broadly studied in the remediation of oil-contaminated water due to their high efficiency and accuracy in the separation of particles [25-28]. However, their manufacturing can be expensive and sometimes complicated. It has been investigated that decorating graphene oxide nanosheets using silica nanoparticles can improve the adsorption properties of graphene oxide nanosheets [29].

Interestingly, conductive polymers can be great candidates to produce polymer nanocomposites for various applications such as photocatalysts, energy storage, adsorbents, and so on. One of the most applicable conductive polymers is polyaniline (PANI). PANI has been broadly used as an adsorbent because of its different dopants. The ease of synthesis, environmentally friendly nature, and modulating properties of PANI have made it an attractive candidate for the degradation of organic dyes. Due to its inherent advantages, many researchers have been

investigating PANI-based nanocomposites for different purposes, according to the literature [30]. More details of separation principles using nano adsorbents can be found in the literature [31].

The present study aimed to consider and compare the possible application of PANI-SiO_2 and rGO-SiO_2 nanocomposites to demulsify oil in water emulsion, which has not yet been investigated according to the literature. For this purpose, PANI-SiO_2 and rGO-SiO_2 nanocomposites have been synthesized by applying in situ oxidative polymerization and sol-gel processes, respectively. The possible application of PANI-SiO_2 and rGO-SiO_2 to oily water treatment has not yet been investigated according to the literature. The synthesized nanocomposites were characterized by applying Fourier transform infrared (FTIR), scanning electron microscopy (SEM), and X-ray diffraction (XRD). The demulsification efficiency of the PANI-SiO_2 and rGO-SiO_2 were evaluated by using a UV Spectrophotometer to determine the oil content in the separated water. In addition, the bottle test and optical observation were applied to evaluate the demulsification performance of PANI-SiO_2 and rGO-SiO_2. According to the obtained results, the hydrophobicity property of the PANI-SiO_2 was better than that of the rGO-SiO_2, which led to better separation efficiency. Furthermore, PANI-SiO_2 and rGO-SiO_2 nanocomposites performed as excellent demulsifiers to quickly separate the oil from the O-W emulsion within a few minutes with no more energy consumption.

EXPERIMENTAL PROCEDURE

Materials

Chemicals applied in this work include Tetraethylorthosilicate (TESO, 99.9%, Merck), absolute ethanol (EtOH 99.5%), acetic acid (S.D. Fine), PVP (LOBA), ammonia (NH_3 25%), deionized water, aniline monomer (99.5 %), ammonium persulfate (APS), HCl, H_2SO_4, $NaNO_3$, H_2O_2 (30%), $NaBH_4$, Tetraorthosilicates (TEOS), (all purchased from Merck). GO nanosheets were synthesized from graphite powder graphite (purchased from Arak Petrochemical Company) by the use of a modified Hummers method [32].

Synthesis of SiO_2 nanoparticles

SiO_2 nanoparticles have been synthesized using the sol-gel method [33]. A mixture of 5 ml of TEOS with 30 ml of absolute ethanol was provided and stirred for 10 min at room temperature. Then, 1 ml of deionized water was added dropwise into the reaction chamber to facilitate the hydrolysis process of TEOS. After that, 2.5 ml of ammonia was fed into the chamber at the rate of 0.01 ml/min. The gel was formed after 1 h and transformed to gel after 24 hrs. Eventually, to obtain nanoparticles, the gel was dried for 2 hrs at 100 ^oC and calcined at 500 ^oC for 3 hrs using a conventional oven. The resultant was ground to get SiO_2 nanoparticles.

Graphene oxide (GO) synthesis

A GO suspension was composed of graphite powder (purchased from Arak Petrochemical Company) using a modified Hummers method. As a brief explanation of the experimental procedure, at first, 120 ml of H_2SO_4 with 0.5 g of $NaNO_3$ were stirred in a 500 ml flask at less than 5 ^oC ice bath. Next, graphite powder, $KMnO_4$ solution, and deionized water (250 ml) were simultaneously and gradually added under blending while the reaction temperature was controlled below 20 °C for 2 hrs. After increasing the temperature to 30 °C, excess deionized

water (700 ml) was added to the mixture, and at the same time, 10 ml H_2O_2 was added while the temperature was increased to 90 ºC until the reaction completed and the color of the combination converted to brilliant yellow (it took about 12 hrs). After cooling to ambient temperature, the black homogeneous dispersion was precipitated by centrifugation and dried under vacuum at 60 ºC for 12 hrs. The resultant was graphene oxide nanosheets [34].

Reduction of GO to rGO

The thermal reduction was applied as a clean method to omit oxygenated functional groups from GO surfaces to produce rGO. For this purpose, a mixture of 0.1 g of synthesized GO, 0.3 g of $NaBH_4$, and 30 ml of water was prepared and sonicated for 1 hr. The resultant was refluxed at 100 ºC for 10 hrs under homogenous agitating. After changing the color of GO from brown to black, it was separated in a centrifuge, washed, and dried at 100 ◦C for 24 hrs.

Synthesis of PANI-SiO_2 nanocomposite

For this purpose, an in-situ polymerization process was applied [35, 36]. 150 mg of silica nanoparticles were added to 50 ml of deionized water under ultrasound. A solution of 0.04 mol/l of aniline was added with a pH of 3.5 which was stabilized by adding HCl 1M solution. In this case, the ratio of silica to aniline was about 0.8. To adsorb anilinium cation onto silica particles, the provided mixture was stirred for 100 min at 21 ºC. Then, 2 ml of APS solution was added dropwise as an oxidant to complete the polymerization reaction and a green color was observed. The precipitated resultant was washed using ethanol and distilled water and dried at 80 ºC for 15 hrs.

Synthesis of rGO-SiO_2 nanocomposite

The nanocomposite was prepared by the use of the sol-gel method [37, 38]. A mixture of 100 g of rGO, 1.7 g of TEOS, and 10 ml ethanol using sonicate bath was prepared. The solution was mixed for 10 min in an oil bath at 40 ºC. To complete the reaction, 0.3 g ammonia was abruptly added and the mixture was stirred for 16 hrs at room temperature. The resultant was separated by 8000 rpm centrifugation, washed with ethanol and distilled water, and then dried at 70 ºC for 24 hrs. Finally, it was calcined at 500 ºC to obtain the porous nanocomposite.

CHARACTERIZATION METHODS

The structures of PANI-SiO_2 and rGO-SiO_2 were determined by an X-ray diffractometer (made by Shimadzu, 1600 model) with specifications of 20 kV, 15 mA, and Cu-Kα radiation of a wavelength of 1.54 Å. The surface morphology of GO, rGO, PANI/SiO_2, and rGO/SiO_2 was determined by applying a scanning electron microscope (SEM, made by ZEISS, EVO 15 model) operating at 15 kV. UV-Vis was applied to determine the amount of oil in the separated water (UV-1700 model made by Shimadzu). The compositional analysis of the GO and rRGO was performed by applying an energy-dispersive X-ray (EDX) spectroscope (Shimadzu, 7000 model). The surface area and the pore size distribution of the samples of PANI-SiO_2 and rGO-SiO_2 were analyzed by BET (made by JWGB, JW-DA model).

RESULTS AND DISCUSSION

XRD characterization

The crystalline structure of the different nanocomposites was characterized through X-ray diffraction (XRD) and the spectra are shown in Fig. 1. Specimens (PANI-SiO_2 and rGO-SiO_2) were scanned in the angle range (2θ) of 20° to 80°. The sharp peaks were observed in both spectra. Two peaks at the points of 2θ = 45° and 67° for both spectra corresponded to SiO_2. The peaks obtained at 2θ = 27.37° and 2θ = 28.45° in the spectra indicated the characterization of polyaniline and reduced graphene oxide, respectively. A slight difference between the XRD spectra of PANI-SiO_2 and rGO-SiO_2 was observed, which was in agreement with the literature [33, 34]. The average particle size of rGO-SiO_2 and PANI-SiO_2 was calculated by the Scherrer formula, as stated below [37].

$$D = \frac{0.9\lambda}{\alpha\cos\theta} \qquad (1)$$

which D is the average crystallite size of the powdered particles, λ = 1.54 Å is the wavelength of CuKα, α is full width at half maximum of the intensity of the major peak, θ is the angular position of the peak. The crystallite sizes of the PANI-SiO_2 and rGO-SiO_2 nanoparticles were estimated to be 0.04 nm and 0.1 nm respectively, which indicated that the specific surface area of PANI-SiO_2 was more than that of the rGO-SiO_2. It can be accordingly deduced that the adsorption capability of PANI-SiO_2 can be more prominent.

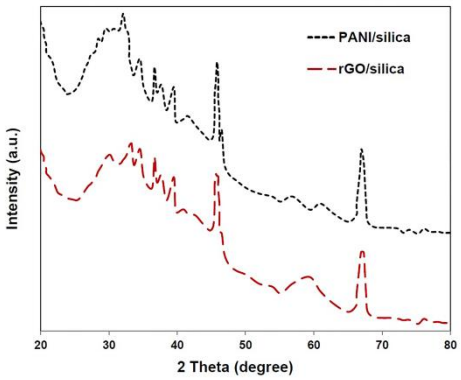

Fig. 1. XRD spectra of PANI-SiO_2 and rGO-SiO_2.

FTIR analysis

The FTIR spectra of PANI, PANI-SiO_2, rGO, and rGO-SiO_2 are indicated in Fig. 2. It can be seen that the spectra of nanocomposites contain all the main characteristic bands. There are some significant peaks in the FTIR spectra of nanocomposites that confirm their successful formation. For PANI and PANI-SiO_2 a (Figure 2 (a) and (b)), the peak in the range of 1600-1500 1/cm shows the stretching modes of C=N and C=C, while the peak in the range of 1300-1250 1/cm corresponds to C–N mode of the benzenoid ring, and the band at 1106 1/cm reveals the bending vibration of C–H mode which is appeared during protonation [39, 41]. There is a difference between PANI and PANI-SiO_2 spectra, which were observed at 1106 and 1108 1/cm. It indicates remarkable interactions between PANI and silica. For rGO and rGO-SiO_2 (Figure 2 (c) and (d)), the extensive peak at 3438 1/cm corresponds to vibrations of the hydroxyl group of water. According to the rGO spectrum, the peak at 1421 1/cm is assigned to the aromatic group (C=C bond) and carbonyl and carboxyl moieties groups (C-O bonds) of rGO [32, 40]. With a comparison between rGO and rGO-SiO_2 spectra, new peaks at 1084, 780, and 460 1/cm can be observed. These

peaks were assigned to symmetric and asymmetric stretching of vibrated modes of Si-O-Si bonds, which related to integrated SiO_2 on the surface of rGO sheets.

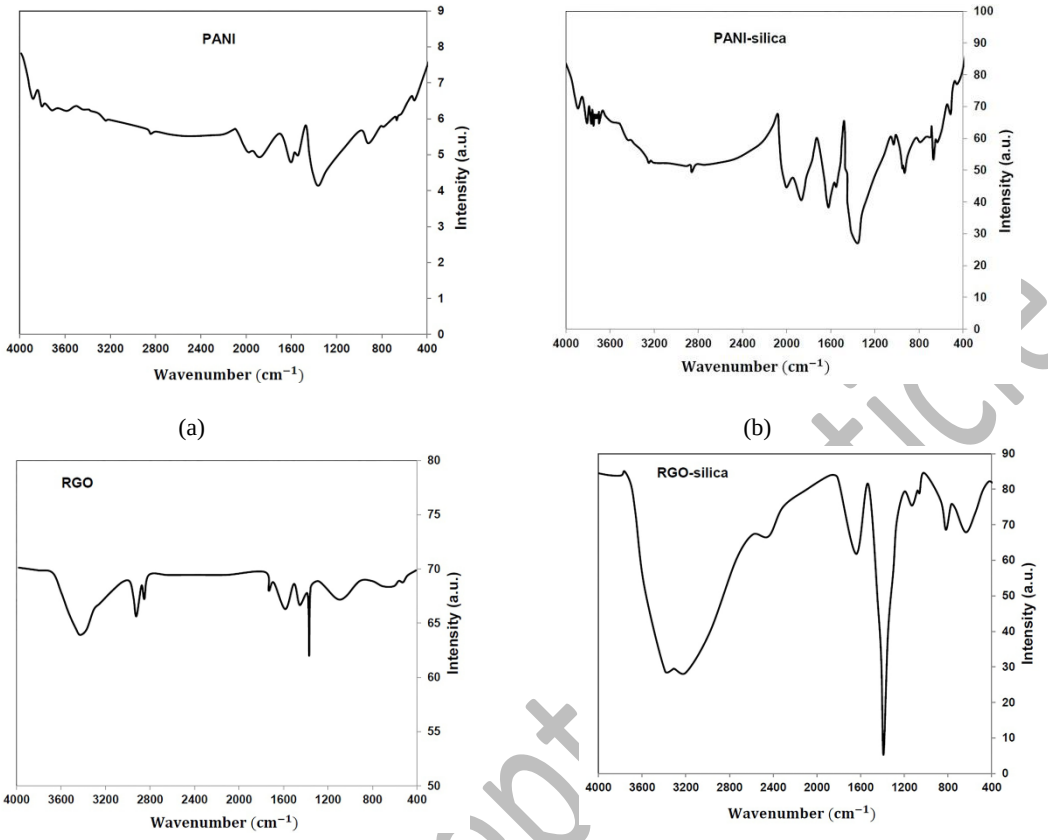

Fig. 2. FTIR spectra of (a) PANI, (b) PANI-SiO_2, (c) rGO, (d) rGO-SiO_2.

SEM analysis

The SEM test was applied to study the structural and morphological specifications of GO, rGO, PANI-SiO_2, and rGO-SiO_2 (Figs. 3 and 4). In addition, the EDX test was performed for compositional analysis. The SEM images revealed that the GO and rGO nanosheets were uniformly formed on the surface, with some detected wrinkles and folds due to accumulated thin nanosheets (Fig. 3 (a) and (b)). The results not only confirmed that two-dimensional nanosheets of GO can be produced from GO exfoliation but also indicated that thermal annealing led to a similar morphology of the resulting rGO flakes in comparison with GO. Reported results in some literature validate it [42, 43]. Furthermore, the EDX analysis confirmed a reduction in oxygen mass and an increase in the carbon mass of rGO (with a mass ratio of C:O equal to 12:5) in comparison with GO (with a mass ratio of C:O equal to 5:8). The surface analysis of SiO_2, PANI/SiO_2, and rGO-SiO_2 was obtained and presented in Fig. 4. It can be seen that the PANI-SiO_2 nanocomposite was characterized by less agglomeration in comparison with the rGO-SiO_2 nanocomposite. The SiO_2 nanoparticles are finely dispersed into a polymer matrix and precipitated on the surfaces of rGO flakes and PANI nanocomposites.

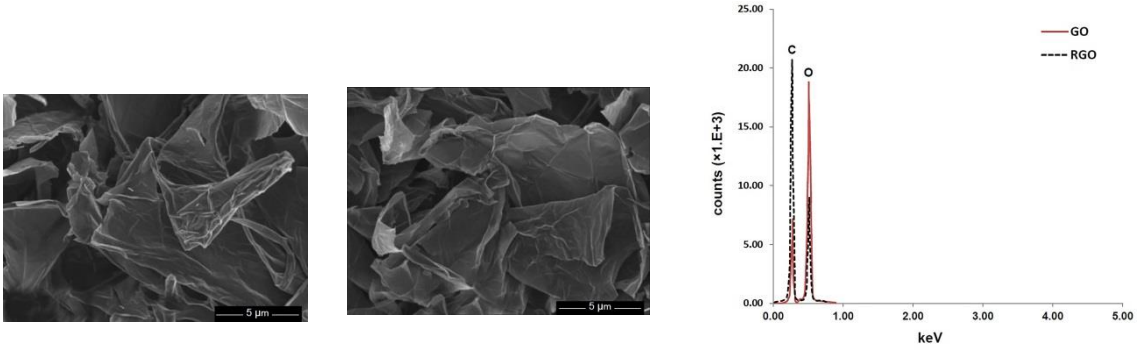

(a) (b) (c)

Fig. 3. SEM images of (a) GO, (b) rGO, (c) EDX analysis.

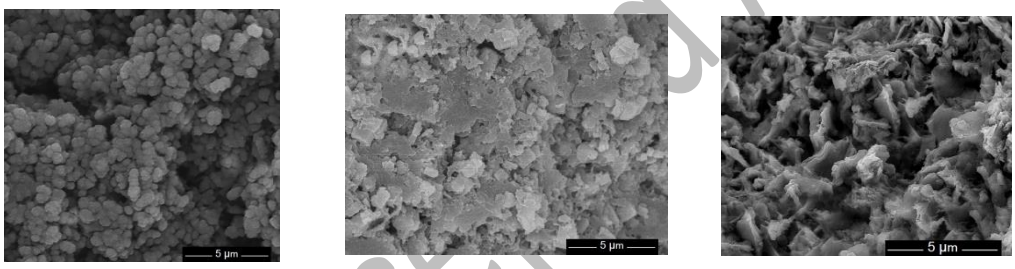

(a) (b) (c)

Fig. 4. SEM images of (a) SiO_2, (b) PANI-SiO_2, (c) rGO-SiO_2.

Hydrophobicity observations of prepared nanocomposites

The hydrophobicity properties of rGO-SiO_2 and PANI-SiO_2 have been determined, as shown in Fig. 5. It was observed that the contact angles for PANI-SiO_2 and rGO-SiO_2 were 124±1° and 134±1°, respectively. The hydrophobicity of both nanocomposites was considerable, while it was better for PANI-SiO_2. This phenomenon may be explained by the small number of oxygenated groups (based on the FTIR spectra) on the surface of rGO-SiO_2 nanocomposite, which increases its hydrophilic tendency. Silica content can increase the hydrophobic tendency of the nanocomposites, as observed. Silica can also supply abundant hydrophobic groups, resulting in more hydrophobic surfaces. As a result, the better hydrophobicity potential of nanocomposite offers possibilities for application in the O-W emulsion separation process.

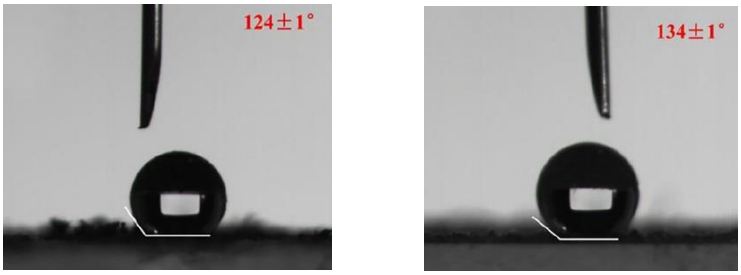

(a) (b)

Fig. 5. Water droplet contact angle on (a) PANI-SiO_2 and (b) rGO-SiO_2.

Brunauer-Emmett-Teller (BET) surface area and pore size analyses

To determine the surface area and pore size of prepared nanocomposites, BET analysis has been carried out, and the results are shown in Fig. 6. According to Fig. 6 (a), the IV isotherm indicates the mesoporous structure of specimens. The measured surface area of PANI-SiO_2 was approximately 36 m^2/g, which is about two times larger compared to that of rGO-SiO_2 (16 m^2/g). In addition, the cumulative pore volume of both specimens is shown in Fig. 6 (b). As can be seen, a higher pore volume is observed for the PANI-SiO_2 nanocomposite compared with pure rGO-SiO_2, which corresponds to a more porous morphology. As a result, the higher active surface area of PANI-SiO_2 causes higher adsorption efficiency.

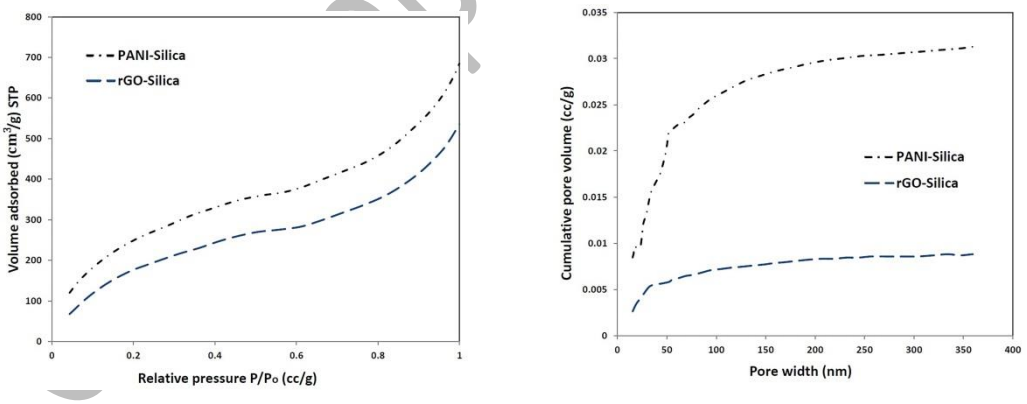

(a) (b)

Fig. 6. (a) Isotherm and (b) cumulative pore volume for PANI-SiO_2 and rGO-SiO_2.

Demulsification evaluation

Firstly, a 2 mg/ml suspension of each nanocomposite was prepared and dispersed in 40 ml of O-W emulsion. It is worth mentioning that the dosage of each nanocomposite in the demulsification process can be calculated using the mass concentration of the nanocomposite in the emulsion. The final solution was properly stirred inside capped cylinders for a few minutes to make a well-mixed emulsion. To observe the O-W separation, the cylinders were placed under ambient conditions. The cylinder containing water was used as a reference. To determine the amount of residual oil in the O-W emulsion, a UV-Vis spectrophotometer at 1 cm path length was utilized. The oil concentration in separated water specimens was calculated by the following equation [44]:

$$C_o = \frac{m_o}{V_w} \times 10^3 \qquad (2)$$

where C_o (mg/l) is the oil concentration, m_o (mg) is the mass of oil in the standard curve, and V_w (ml) is the water volume. The demulsification efficiency can be calculated using the following equation:

$$E = \frac{C_o - C_i}{C_o} \times 100 \qquad (3)$$

where E is the demulsification efficiency (%), C_o is the initial amount of oil (mg/l) in the emulsion, and C_i is the residual amount of oil in the separated water.

Demulsification performance of PANI-SiO_2 and RGO-SiO_2

To evaluate the performance of the synthesized nanocomposites in the demulsification process, a bottle test was provided (Fig. 7 (a)-(d)). All bottles contained the same volume of emulsion (50 g/l). Figs. 7 (a) and 7 (b) corresponded to the demulsification process applying rGO-SiO_2, and Figs 7 (c) and 7 (d) corresponded to the demulsification process applying PANI-SiO_2, respectively. After adding a small amount of two different nanocomposites, the stability of the emulsion instantaneously collapsed, and the O-W separation process was expedited by the coalescence of the oil droplets, as can be seen in the figures. Accordingly, the condensed oil phase and colorless water phase were observed, which indicated a simple, fast, and highly efficient demulsification process. Both the synthesized nanocomposites showed considerable demulsification efficiency, while the performance of the PANI-SiO_2 nanocomposite was better, as observed in Fig. 6. To support that claim, optical microscopy images have been provided, as shown in Fig. 6.

Fig. 8 (a) is related to the first 60 seconds of the demulsification process for both nanocomposites. The agglomeration of oil droplets was completely observed. After giving enough time to the process (a few minutes), it was observed that the separated oil phase was purer and included fewer water droplets when applying PANI-SiO_2 in comparison with rGO/SiO_2. It can be explained that the spongy matrix of PANI-SiO_2 has a better adsorbent ability because of the finely dispersed SiO_2 nanoparticle in the polymer matrix and its well-designed hydrophobic character.

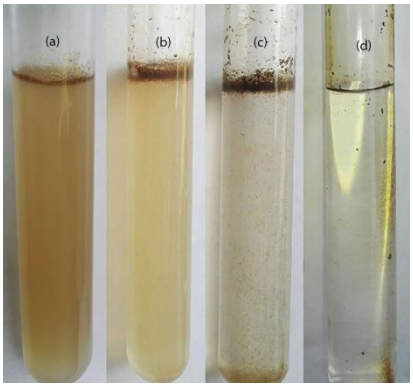

Fig. 7. (a) and (b) demulsification process using rGO-SiO_2 after 60 and 120 seconds, respectively. (c) and (d) demulsification process using PANI-SiO_2 after 60 and 120 seconds, respectively.

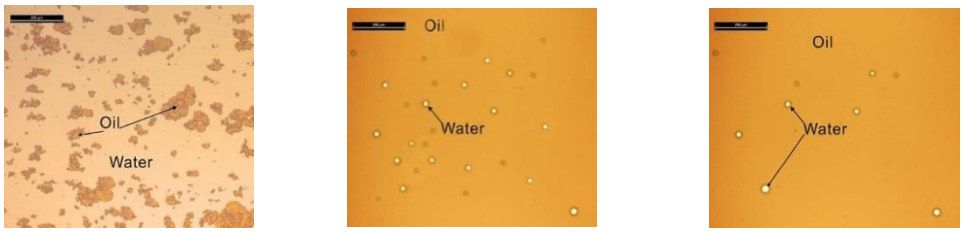

(a) (b) (c)

Fig. 8. Optical microscopy images (a) the first 60 seconds of the demulsification process regarding both nanocomposites. (b) the first 120 seconds of the demulsification process using rGO-SiO_2. (c) the first 120 seconds of the demulsification process using PANI-SiO_2.

Effect of adsorbent dosage on demulsification

To explore the performance of two different nanocomposites in the demulsification process, two O-W emulsions with two different percentages of oil in water (50 g/l and 5 g/l) were prepared. Furthermore, a comparison between the performances of the synthesized nanocomposites and porous graphene oxide (GO) nanosheets [45] has been carried out. The demulsification process took 2 minutes for both synthesized nanocomposites. The demulsification efficiency of the nanocomposites was determined by applying a UV spectrophotometer to estimate the amount of oil in the separated water. It was figured out that the nanocomposites could acceptably demulsify both emulsions as shown in Figs. 9 (a) and 9 (b). In addition, the results revealed that the optimum dosage of the nanocomposites in the demulsification process can be changed according to the amount of oil in the O-W emulsion. It was observed from the results that the maximum demulsification efficiency can be obtained when the amount of oil in the O-W emulsion is lower. Increasing the dosage of the nanocomposites over a threshold could contribute to a slight increase in the amount of oil in the separated water. This eccentric phenomenon can likely be attributed to the distribution of nanocomposite sheets after demulsification. When the amount of adsorbents increases in the water phase, the adsorbed oil on the adsorbent surface causes a slight increase in the amount of oil in the separated water [46].

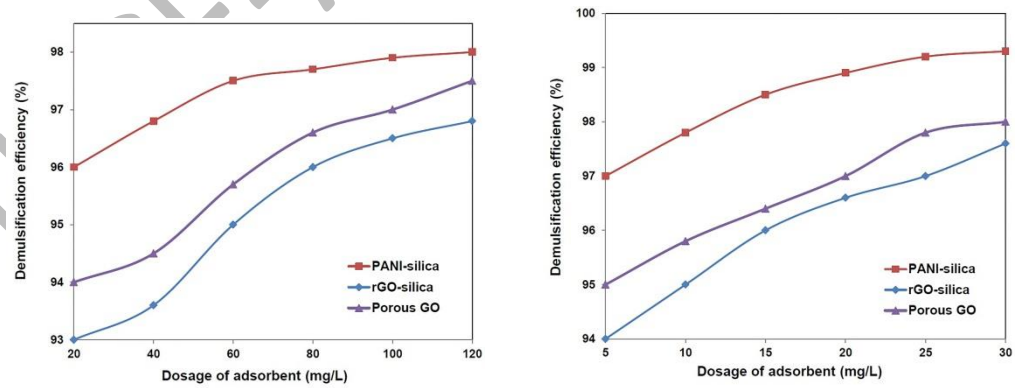

(a) (b)

Fig. 9. De-emulsification efficiency of PANI-SiO_2, rGO-SiO_2, and porous GO as a function of adsorbent dosage for (a) 50 g/l and (b) 5 g/l of oil in water emulsion.

It was also figured out that the absorbent capability of PANI-SiO_2 was higher than that of rGO-SiO_2 and porous GO due to its higher specific surface area and demulsification efficiency. According to the results, the adsorption capacity of porous GO was higher compared to the rGO-SiO_2 nanocomposite. It can be explained by the presence of more chemical agents (carbonyl, hydroxyl, and ethoxy on the edges of GO) and a higher surface area of GO in comparison with rGO [45]. The results indicated that the optimum dosages of PANI-SiO_2 and rGO-SiO_2 are closely associated with the oil content of the emulsion. As shown in Figure 9, the demulsification efficiency increases with increasing the adsorbent dosage for both nanocomposites. Furthermore, after reaching a threshold of adsorbent dosage, the demulsification efficiency decreased due to the distribution of nanocomposites after demulsification. In addition, the oil demulsification efficiency increases for the emulsion with an oil content of 5 g/l rather than 50 g/l for both adsorbents, which can be explained due to the more saturated surface of the adsorbent, the less demulsification efficiency of the adsorbent. Consequently, the required adsorbent decreases in the emulsion with a lower oil content. It can be concluded from the obtained results that PANI-SiO_2 showed better sponge behavior compared to rGO-SiO_2 and porous GO and, accordingly, better performance in the purification of oil-contaminated water. All these results suggest that applying the synthesized nanocomposites can be a promising approach to separating oil in water emulsion.

Possible demulsification mechanism

O-W emulsion usually consists of molecules of asphaltenes, resins, and naphthenic acids. These molecules generate a repulsive force of the electrical double layer with oil droplets (a protective film) which causes the stability of O-W emulsion [47, 48]. Breaking up this protective film is a key to an efficient demulsification process. The synthesized nanocomposites (adsorbents) have both hydrophilic and hydrophobic edges which make a good dispersion in the water phase. When the adsorbent is added to the O-W emulsion, the adsorbent particles reach the O-W interface and partially destroy the protective film which provides a side to the coalescence of the small droplets to create bigger droplets. Correspondingly, the oil successfully separates from the water phase [42]. The adsorption performance of the synthesized nanocomposites confirmed a proper interaction between oil and adsorbent particles.

The possible mechanism of adsorption of oil droplets on the surface of nanoparticle adsorbers (for instance GO, rGO, PANI-SiO_2, rGO-SiO_2, and so on) can be explained as shown in Figure 10 [49]. Figure 8 indicates the schematic mechanism of oil droplet adsorption on the surface of GO nanosheets. After adding GO nanosheets into the O-W emulsion, the nanosheets diffused uniformly in the water phase to reach the active surfaces of molecules (Fig. 10 (a2) and (b2)). Forming a strong interaction between nanosheets and oil droplets led to the destruction of the protective film (Fig. 10 (b3)), which generated coalescence sites for smaller oil droplets to grow. Consequently, it leads to oil phase formation (Fig. 10 (a3)). The oil is eventually separated from the water phase. This mechanism has also been reported in some literature [50-52]. It has been also suggested that the increase in the absorption capacity enables a $\pi - \pi$ interaction between the GO and the asphaltenes leading to easier disruption of the interfacial film. This eventually promoted oil droplets to coalesce and enhanced the separation of oil from water. More details regarding the demulsification mechanism and $\pi - \pi$ interaction between nanocomposite as an adsorbent and oil particles can be found in the literature [53].

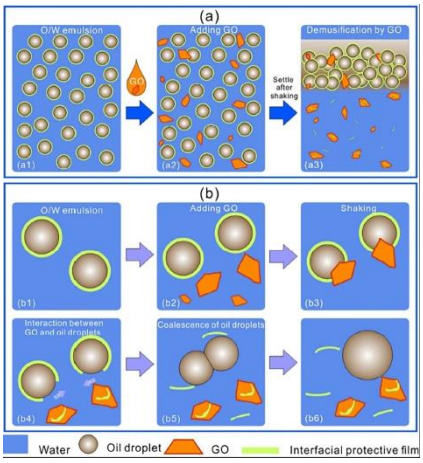

Fig. 10. Schematic illustration of the demulsification processes and the possible mechanism for the coagulation of the oil droplets driven by the GO nanosheets [49].

CONCLUSIONS

Recently, nanoparticles and polymeric nanoparticles have received great interest in the adsorption process, especially in wastewater treatment, due to their high specific surface area. One of the most challenging issues concerning the environment is oily wastewater, which should be taken into account. In this study, the performance of two organic and inorganic nanocomposites in the separation of oil from oil in a water emulsion has been investigated. SiO_2 nanoparticles have shown considerable potential in adsorption processes. Therefore, in this comparative study, PANI- SiO_2 and rGO- SiO_2 were synthesized using in-situ polymerization and sol-gel processes, respectively. The synthesized nanocomposites were characterized by applying XRD, SEM, and FTIR tests. In addition, a UV-Vis analysis was performed to determine the amount of oil in the separated water. After preparing two different O-W emulsions and demulsifying using the synthesized nanoparticles as adsorbents, the results revealed that the capabilities of both nanocomposites were significant. Moreover, a better surface characterization (according to SEM, BET, and hydrophobicity analyses) for PANI-SiO_2 was observed, suggesting better adsorption performance of oil from the O-W emulsion. The results of demulsification efficiency showed that it closely corresponded to the amount of oil in the O-W emulsion, which was independent of the adsorbent type. According to the optical microscopy images and bottle test, it was proven that the demulsification efficiency of the PANI-SiO_2 nanocomposite was higher than that of rGO-SiO_2 for both O-W emulsions which can be attributed to the high specific surface area and better sponge behavior of PANI-SiO_2. An optimum amount of adsorbent was observed, which indicated that there was a threshold for the dosage of adsorbent. Therefore, it should be noticed in practical conditions. The possible adsorption mechanism of oil on the nanocomposite surface can be explained by $\pi - \pi$ interaction between the adsorbent and oil particles, which has been described in detail in the literature. A comparison between prepared nanocomposites and porous GO nanosheets in O-W demulsification revealed that the adsorption capacity of PANI-SiO_2 was more significant in comparison with the mentioned nanocomposites in the O-W separation process. Therefore, it can be a promising alternative to industrial wastewater treatment.

REFERENCES

[1] Atta A.M., Al-Lohedan H.A., Abdullah M.M.S., Dipoles Poly (ionic liquids) Based on 2-acrylamido-2-methylpropane Sulfonic acid-co-hydroxyethyl Methacrylate for Demulsification of Crude Oil-water Emulsions. *Journal of Molecular Liquids*, **222:** 680-690 (2016).

[2] Chen Z., Peng J., Ge L., Xu Z., Demulsifying Water-in-oil Emulsions by Ethyl Cellulose Demulsifiers Studied Using Focused Beam Reflectance Measurement, *Chemical Engineering Science*, **130:** 254-263 (2016).

[3] Kang W., Guo L., Fan H., Flocculation, Coalescence and Migration of Dispersed Phase Droplets and Oil-water Separation in Heavy Oil Emulsion. *Journal of Petroleum Science and Engineering*, **81:** 177-181 (2012).

[4] Lv X., Song Z., Yu J., Su J., Study on the Demulsification of Refinery Oily Sludge Enhanced by Microwave Irradiation, *Fuel*, **279:** 118417 (2020).

[4] Shi C., Zhang L., Xie L., Liu Q., He J., Mantilla C.A., Surface Interaction of Water-in-oil Emulsion Droplets with Interfacially Active Asphaltenes, *Langmuir*, **33 (5):** 1265-1274 (2017).

[5] Sokker H.H., El-Sawy N.M., Hassan M.A., El-Anadouli B.E., Adsorption of Crude Oil from Aqueous Solution by Hydrogel of Chitosan Based Polyacrylamide Prepared by Radiation-induced Graft Polymerization. *Journal of Hazardous Materials*, **190 (3):** 359-365 (2011).

[6] Srinivasan A., Viraraghavan T., Ng K.T.W., Coalescence/Filtration of an Oil-In-Water Emulsion in an Immobilized Mucor rouxii Biomass Bed. *Separation Science and Technology*, **47 (16):** 2241-2249 (2012).

[7] Li H., Mu P., Li J., Wang Q., Inverse Desert Beetle-like ZIF-8/PAN Composite Nanofibrous Membrane for Highly Efficient Separation of Oil-in-water Emulsions. *Journal of Mater Chemistry A*, **9 (7):** 4167-4175 (2021).

[8] Fan C., Ma R., Wang Y., Luo J., Demulsification of Oil-in-Water Emulsions in a Novel Rotating Microchannel, *Industrial and Engineering Chemist Research*, **59 (17):** 8335-8345 (2020).

[9] Dhandhi Y., Chaudhari R.K., Naiya T.K., Development in Separation of Oil Field Emulsion Toward Green Technology: A Comprehensive Review, *Separation Science and Technology*, **57 (10):** 1–27 (2021).

[10] Atta A.M., Fadda A.A., Abdel-Rahman A.A.H., Application of New Modified Poly(ethylene Oxide)- Block-Poly(propylene oxide)-Block-Poly(ethylene oxide) Copolymers as Demulsifier for Petroleum Crude Oil Emulsion. *Journal of Dispersion Science and Technology*, **33 (6):** 775-785 (2012).

[11] Dalmazzone C., Noik C., Komunjer L., Mechanism of Crude-oil/water Interface Destabilization by Silicone Demulsifiers. *SPE Journal*, 10 (1): 44-53 (2006).

[12] Zhang L., Ying H., Yan S., Zhan N., Guo Y., Hyperbranched poly(amido amine) Demulsifiers With Ethylenediamine/1,3- propanediamine as an Initiator for Oil-in-water Emulsions with Microdroplets. *Fuel*, **226:** 381-388 (2018).

[13] Hao L., Jiang B., Zhang L., Efficient Demulsification of Diesel-in-water Emulsions by Different Structural Dendrimer-based Demulsifiers, *Industrial and Engineering Chemist Research*, **55 (6):** 1748-1759 (2016).

[14] Jabbari M., Izadmanesh Y., Ghavidel H., Synthesis of Ionic Liquids as Novel Emulsifier and Demulsifiers, *Journal of Molecular Liqduids*, **293:** 111512 (2019).

[15] Zolfaghari R., Fakhru'l-Razi A., Abdullah L.C., Pendashteh A., Demulsification Techniques of Water-in-oil and Oil-in-water Emulsions in Petroleum Industry. *Separation and Purification Technology*, 170: 377-407 (2016).

[16] Liu J., Wang H., Jia X., Recyclable Magnetic Graphene Oxide for Rapid and Efficient Demulsification of Crude oil-in-water Emulsion. *Fuel*, **189:** 79-87 (2017).

[17] Nikkhah M., Tohidian T., Rahimpour M.R., Jahanmiri A., Efficient Demulsification of Water-in-oil Emulsion by a Novel Nano-titania Modified Chemical Demulsifier, *Chemical Engineering Research and Design*, **94:** 164–172 (2015).

[18] Zhang J., Li Y., Bao M., Wang Z., Facile Fabrication of Cyclodextrin-Modified Magnetic Particles for Effective Demulsification from Various Types of Emulsions, *Environmental Science and Technology*, **50 (16):** 8809-8816 (2016).

[19] Liu J., Li X., Jia W., Li Z., Demulsification of Crude Oil-in-Water Emulsions Driven by Graphene Oxide Nanosheets, *Energy Fuels*, **29 (7):** 4644-4653 (2015).

[20] Wang H., Liu J., Xu H., Ma Z., Demulsification of Heavy Oil-in-water Emulsions by Reduced Graphene Oxide Nanosheets. *RSC Advances*, **6:**106297-106307 (2016).

[21] McCoy T.M., Turpin G., Teo B.M., Tabor R.F., Graphene Oxide: a Surfactant or Particle?, *Current Opinion in Colloid and Interface Science*, **39:** 98-109 (2019).

[22] Hidayati Othman N., Fadhil Jahari A., Alias N.H., Demulsification of Crude Oil in Water (O/W) Emulsions using Graphene Oxide, *IOP Conference Series: Materials Science and Engineering*, **458:** 1-7 (2018).

[23] Dalvand A., Asleshirin S., Fallahiyekta M., Hydrophobic Silica Nanoparticle and Anionic/Cationic Surfactants Interplays Tailored Interfacial Properties for the Wettability Alteration and EOR Applications, *Iranian Journal of Chemistry and Chemical Engineering*, **41 (3):** 1076-1094 (2022).

[24] Rajabi Ghaleh V., Mohammadi A., The Stability and Surface Activity of Environmentally Responsive Surface-Modified Silica Nanoparticles: the Importance of Hydrophobicity, *Journal of Dispersion Science and Technology*, **41 (9):** 1299-1310 (2020).

[25] Noamani S., Niroomand S., Rastgar M., Sadrzade M., Carbon-based Polymer Nanocomposite Membranes for Oily Wastewater Treatment, *npj Clean Water*, **2:** 1-14 (2019).

[26] Ezugbe E.O., Rathilal S., Membrane Technologies in Wastewater Treatment: a Review, *Membranes*, **10 (5):** 1-28 (2020).

[27] Nouf A.H., Mervette E.B., Elewa M.M., Prospects of Polymeric Nanocomposite Membranes for Water Purification and Scalability and their Health and Environmental Impacts: a Review, *Nanomaterials*, **12 (20):** 3637-3682 (2022).

[28] Antolín-Cerón V.H., González-López F.J., Astudillo-Sánchez P.D., High-Performance Polyurethane Nanocomposite Membranes Containing Cellulose Nanocrystals for Protein Separation, *Polymers*, **14 (4):** 831-846 (2022).

[29] Cijun Shuai F.Y., Yang. S., Silicon Dioxide Nanoparticles Decorated on Graphene Oxide Nanosheets and Their Application in Poly(l-lactic acid) Scaffold, *Journal of Advanced Research*, **48:** 175–190 (2023).

[30] Babakhani D., Hamidi M., Possible Application of Ternary Polyaniline-Graphene-Montmorillonite Nanocomposite for Electromagnetic Pollution Shielding, *Iranian Journal of Chemistry and Chemical Engineering*, accepted manuscript, (2023).

[31] Liang H., Esmaeili H., Application of Nanomaterials for Demulsification of Oily Wastewater: a Review Study, *Environmental Technology & Innovation*, **22:** 101498 (2021).

[32] Zaabaa N.I., Foo K.L., Hashim U., Synthesis of Graphene Oxide using Modified Hummers' Method: Solvent Influence, *Procedia Engineering*, **184:** 469-477 (2017).

[33] Hintze C., Morita K., Riedel R., Mera G., Facile Sol–gel Synthesis of Reduced Graphene Oxide/silica Nanocomposites, *Journal of the European Ceramic Society*, **36 (12):** 2923-293 (2016).

[34] Badieia E., Sangpour .P, Bagheria M., Pazouki M., (2014) Graphene Oxide Antibacterial Sheets: Synthesis and Characterization, *International Journal of Engineering Transactions C: Aspects*, **27 (12):** 1803-1808.

[35] Kim M., Cho S., Song J., Son S., Jang J., Controllable Synthesis of Highly Conductive Polyaniline Coated Silica Nanoparticles Using Self-Stabilized Dispersion Polymerization, *ACS Applied Material & Interfaces*, **4(9):** 4603-4609 (2014).

[36] Sofyan N., Nugrahaa R.A., Ridhovaa A.,Yuwono H., Characteristics of PANi/rGO Nanocomposite as Protective Coating and Catalyst in Dye-sensitized Solar Cell Counter Electrode Deposited on AISI 1086 Steel Substrate, *International Journal of Engineering Transactions A: Basics*, **31 (10):** 1741-1748 (2018).

[37] Moslehi Niasara M., Molaei M.J., Aghae A., Electromagnetic Wave Absorption Properties of Barium errite/Reduced Graphene Oxide Nanocomposites, *International Journal of Engineering Transactions C: Aspects*, **34 (6):** 1505-1513 (2021).

[38] Khanmohammadi A., Rashidi V., Sadighian S., Reduced Graphene Oxide/Silica Nanocomposite as Anticancer Drug Delivery Nanocarrier, *Biointerface Research in Applied Chemistry*, **13 (4):** 383-392 (2023).

[39] Ambalagi S.M., Devendrappa M., Nagaraja S., Sannakki B., Dielectric Properties of PANI with Metal Oxide Nanocomposites, *AIP Conference Proceeding*, **1989 (1):** 1-8 (2018).

[40] Devi P.S.R., Synthesis and Characterization of Polyaniline Composites with Silica Gel, Styrene-divinyl Benzene Resin Beads, Calcium Alginate and Tetraethoxy Silane Substrates, *Synthetic Metals*, **276:** 116760 (2021).

[41] Niu Z., Yang Z., Hu Z., Polyaniline–Silica Composite Conductive Capsules and Hollow Spheres, *Advanced Functional Materials*, **13 (12):** 949-954 (2003).

[42] Zaaba N., Foo K., Hashim U., Synthesis of Graphene Oxide Using Modified Hummers Method: Solvent Influence, *Procedia Engineering*, **184:** 469-477 (2017).

[43] Rattana T., Chaiyakun S., Witit-Anun N., Preparation and Characterization of Graphene Oxide Nanosheets, *Procedia Engineering*, **32:** 759-764 (2012).

[44] Muniyalakshmi M., Sethuraman K., Silambarasan D., Synthesis and Characterization of Graphene Oxide Nanosheets, *Materialstoday: Proceeding*, **21(1):** 408-410 (2020).

[45] Nusrat J., Hridoy R., Akter H.R., Arashi S.,Rahman E., a Comparative Study on the Sorption Behavior of Graphene Oxide and Reduced Graphene Oxide Towards Methylene Blue, *Case Studies in Chemical and Environmental Engineering*, **6:** 100232 (2022).

[46] Elhenawy S., Khraisheh M., AlMomani F., Hassan M.K. Selvaraj R., Recent Developments and Advancements in Graphene-Based Technologies for Oil Spill Cleanup and Oil–water Separation Processes, *Nanomaterials*, **12 (1):** 1-25 (2022).

[47] Yingbiao X., Wang Y., Wang T., Demulsification of Heavy Oil-in-Water Emulsion by a Novel Janus Graphene Oxide Nanosheet: Experiments and Molecular Dynamic Simulations, *Molecules*, **27 (7):** 2191-2205 (2022).

[48] Guo J., Liu Q., Li M., The Effect of Alkali on Crude Oil/water Interfacial Properties and the Stability of Crude Oil Emulsions, *Colloids and Surfaces A: Physicochemical and Engineering Aspects*, **273 (1):** 213-218 (2006).

[49] Farooq U., Patil A., Panjwani B., Simonsen G., Review on Application of Nanotechnology for Asphaltene Adsorption, Crude Oil Demulsification, and Produced Water Treatment, *Energy & Fuels*, **35 (23),** 19191-19210 (2021).

[50] Javadian S., Khalilifard M., Sadrpoor S.M., Functionalized Graphene Oxide with Core-Shell of Fe3O4@oliec Acid Nanospheres as a Recyclable Demulsifier for Effective Removal of Emulsified Oil from Oily Wastewater, *Journal of Water Process Engineering*, **32:** 100961 (2019).

[51[Jayakaran P., Nirmala G.S., Govindarajan L., Qualitative and Quantitative Analysis of Graphene-Based Adsorbents in Wastewater Treatment, *International Journal of Chemical Engineering*, 1-17 (2019).

[52] Yonguep E., Kapiamba K.F., Kabamba K.J., Formation M.C., Stabilization and Chemical Demulsification of Crude oil-in-water Emulsions: a Review, *Petroleum Research*, **7 (4):** 459-472 (2022).

[53] Ponnanikajamideen M., Kai H., Tao Z., Malini M., Rajeshkumar S., Efficient Separation of Oil-in-water Emulsions with Functionalized Superhydrophilic Graphene Oxide-Chitosan Based Composite Membrane, *International Journal of Waste Resources*, **11(5):** 1-6 (2021).